Journal of Virological Methods 213 (2015) 151–156

Contents lists available at ScienceDirect

Journal of Virological Methods

journal homepage: www.elsevier.com/locate/jviromet

Diagnosis of human metapneumovirus in patients hospitalized with acute lower respiratory tract infection using a metal-enhanced fluorescence technique

Ying-Feng Chang[a,b], Kuo-Chien Tsao[c,f], Yi-Chun Liu[c], Yu-Chi Chen[a], Pei-Chun Yu[a], Yhu-Chering Huang[d,e], Chien Chou[a,g,*]

[a] Chang Gung University, Graduate Institute of Electro-Optical Engineering, Taoyuan 33371, Taiwan
[b] National Taiwan University, Department of Biochemical Science and Technology, Taipei 10617, Taiwan
[c] Linkou Chang Gung Memorial Hospital, Department of Laboratory Medicine, Taoyuan 33305, Taiwan
[d] Linkou Chang Gung Memorial Hospital, Division of Pediatric Infectious Diseases, Taoyuan 33305, Taiwan
[e] Chang Gung University, College of Medicine, Department of Medicine, Taoyuan 33371, Taiwan
[f] Chang Gung University, College of Medicine, Department of Medical Biotechnology and Laboratory Science, Taoyuan 33371, Taiwan
[g] Chang Gung University, Healthy Aging Research Center, Taoyuan 33302, Taiwan

Article history:
Received 29 August 2014
Received in revised form 4 December 2014
Accepted 5 December 2014
Available online 15 December 2014

Keywords:
Virus detection
Gold nanoparticles
High-throughput biosensor
Localized surface plasmon resonance
Metal-enhanced fluorescence

A B S T R A C T

Human metapneumovirus (hMPV) is a common respiratory tract infection in children. However, conventional immunofluorescence assays (IFAs) for detecting hMPV in respiratory samples have limited reliability with a sensitivity and false-negative predictive value of 58.1% and approximately 17.8%, respectively. In this study, hMPV was measured in 91 clinical respiratory samples (55 sputum and 36 nasopharyngeal aspirate samples), which were obtained from children under three years of age, utilizing our previously developed high-throughput metal-enhanced fluorescence (MEF)-based biosensor (HT-MEFB). The sensitivity of HT-MEFB for hMPV detection in the 91 samples was improved by up to 77.4% compared with that obtained with IFAs, and the specificity of HT-MEFB for hMPV detection was 91.7%. In addition, the specificity and accuracy obtained after the selection of 55 sputum samples as the analyzed specimen reached 92.3% and 90.9%, respectively. Thus, in terms of accuracy, high throughput, and sensitivity, HT-MEFB exhibits considerable potential for hMPV detection in clinical settings.

1. Introduction

Community-acquired pneumonia is a major cause of morbidity and mortality in children because, even with advances in diagnostic tools, the causative agent of 20–30% of upper respiratory tract infections in children is undiagnosed (Janssen et al., 2010). In 2001, Dr. Bernadette van den Hoogen and colleagues first reported the isolation of the paramyxovirus human metapneumovirus (hMPV) from nasopharyngeal aspirate samples from children who suffered from respiratory tract disease (van den Hoogen et al., 2001), and ensuing reports have showed that the clinical symptoms associated with hMPV infection appear to be quite similar to those associated with respiratory syncytial virus (RSV) (Ebihara et al., 2005; Lin et al., 2005; Wei et al., 2013). Although RSV is the most common pathogen and is identified in 43.4% of children with respiratory tract infections, many studies have shown that hMPV is becoming one of the leading causes of pediatric respiratory tract infections (Williams et al., 2004; Huang et al., 2010, 2014).

Currently, there are several methods for the detection of hMPV infections. For example, viral isolation by culture remains the predominant diagnostic method for viral respiratory infections. However, culturing viruses is a labor-intensive procedure and has a long total turnaround time (Kikuta et al., 2008; Kukavica-Ibrulj and Boivin, 2009; Janssen et al., 2010). Enzyme-based immunoassays are another diagnostic method, and commercial enzyme-based immunoassays typically show an acceptable sensitivity (~80%) for hMPV detection (Kukavica-Ibrulj and Boivin, 2009; Janssen et al., 2010; Okamoto et al., 2010). To date, RNA detection by reverse-transcription polymerase chain reaction (RT-PCR) or isothermal amplification technologies (IATs) are the most sensitive

* Corresponding author at: Chang Gung University, Graduate Institute of Electro-Optical Engineering, Taoyuan 33371, Taiwan. Tel.: +886 3 2118800 # 3677; Fax: +886 3 2118507.
E-mail address: cchou01@gamil.com (C. Chou).

http://dx.doi.org/10.1016/j.jviromet.2014.12.005
0166-0934/

and specific procedures for hMPV detection (Ebihara et al., 2004; Landry et al., 2005; Kikuta et al., 2008; Klemenc et al., 2012; Wang et al., 2012). However, IATs are performed only in special laboratories, and RT-PCR requires several hours to obtain results (Landry et al., 2005; Kikuta et al., 2008). The immunofluorescence assay (IFA), which provides results within 2–4 h, is also commonly used in clinical virology laboratories for the diagnosis of respiratory viruses (Ishiguro et al., 2005; Landry et al., 2005, 2008; Ingram et al., 2006; Fenwick et al., 2007). However, IFA not only requires a highly trained technologist to interpret the staining results with the use of a fluorescence microscope but also shows a relatively poor sensitivity of approximately 58.06% in our experimental results. Recently, a gold nanoparticle (GNP)-based immunochromatography assay (ICA) for hMPV detection proposed by Dr. Kikuta et al. showed 70.6% sensitivity and 95.5% specificity, whereas Dr. Matsuzaki et al. showed sensitivity and specificity of 82.3% and 93.8%, respectively.

GNP has been used to improve the detection sensitivity of biosensors because GNP has a high surface-area-to-volume ratio and exhibits unique optical properties, such as localized surface plasmon resonance (LSPR) (Baptista et al., 2008; Chen et al., 2014). In addition, many studies have integrated GNP with a fluorescence technique because GNP can not only produce a localized field that is significantly amplified through LSPR but also make a fluorophore that generates a larger quantum yield of fluorescence emission due to a theoretical increase of at least 1000-fold in the radiative decay rate of the fluorophore (Geddes et al., 2003; Morton et al., 2011). These cause a significantly enhance of the emission of a fluorophore near a GNP compared with that obtained in free-space condition; the phenomenon is so-called metal-enhanced fluorescence (MEF). Based on this technique, we previously developed MEF biosensors to study protein-protein interactions at ultralow concentrations at the pg/mL level (Hsieh et al., 2007; Chang et al., 2009, 2010, 2011, 2013; Huang et al., 2009; Chao et al., 2012). Moreover, the mechanism underlying the fluorescence enhancement using metallic nanoparticles in this biosensor was studied based on the scattering theory (Chang et al., 2009). In this study, hMPV detection using the developed high-throughput MEF-based biosensor (HT-MEFB) was compared to that obtained with RT-PCR and IFA using 91 clinical respiratory samples, including 55 sputum (SP) and 36 nasopharyngeal aspirate samples, all of which were obtained from children under 3 years of age. The sensitivity of HT-MEFB for hMPV diagnosis in all of the specimens was improved up to 77.4% compared with that obtained with IFA, and the specificity of HT-MEFB for hMPV detection was found to be 91.7%. In addition, the selection of only 55 SP samples as the analyzed specimen in this study resulted in specificity and accuracy values of 92.3% and 90.9%, respectively. As a result, in terms of accuracy, high throughput, and detection sensitivity, the HT-MEFB exhibits considerable potential for hMPV diagnosis in clinical settings.

2. Materials and methods

2.1. Clinical samples

This study was approved by the institutional review board of Chang Gung Memorial Hospital (IRB 99-2855B) at Taoyuan, Taiwan. Written consent was obtained from all of the participants. All of the clinical samples were independently obtained from 91 patients under 3 years of age with acute lower respiratory tract infection. A total of 91 patients were recruited from February 2011 to August 2011 in Linkou Chang Gung Memorial Hospital. The 91 specimens included 36 nasopharyngeal aspirate and 55 SP samples, and these were prepared by the Department of Laboratory Medicine, Linkou Chang Gung Memorial Hospital, Taoyuan, Taiwan. Each specimen was collected from a different patient.

Table 1
Primers and probe sequence used for the detection of hMPV.

Primer	Sequence (5′ to 3′)	Size	Position
NLN-forward	5′-CATAYAARCATGCTATATT AAAAGAGTCTC-3′	162 bp	2478–2497
NLN-reverse	5′-CCTATYTCWGCAGCATAT TTGTARTCAG-3′		2558–2537
NLN-probe	5′-FAM-AATGATGARGGTGT CACTG-MGBNFQ-3′		2500–2528

2.2. hMPV detection using the PCR-based assay

The viral RNA from 140 μL of the specimens was extracted using the QIAamp Viral RNA Mini Kit (Qiagen, Valencia, CA, USA) according to the manufacturer's instructions. The RNA was eluted into 30 μL of elution buffer. The resulting RNA (8 μL) was subjected to cDNA synthesis using 50 ng of a random hexamer primer and 500 nM dNTPs. This step was performed at 65 °C for 10 min followed by 4 °C for at least 1 min. An RT mixture containing 1X RT buffer, 10 mM DTT, 40 units of RNaseOut and 200 units of SuperScript III Reverse Transcriptase (Invitrogen, Carlsbad, CA, USA) was applied and cycled at 25 °C for 10 min, 50 °C for 60 min, and 85 °C for 5 min on a BioMetra Thermocycler (Biometra, Goettingen, Germany).

The real-time PCR detection of hMPV was performed using the Bio-Rad CFX96 Touch™ Real-Time PCR Detection System (Bio-Rad, Hercules, CA, USA) with iTaq™ Supermix (Bio-Rad, Hercules, CA, USA). The primers and probe sequence for the detection of hMPV are shown in Table 1. Amplification was performed in a total volume of 20 μL containing 10 μL of 2X iTaq™ Supermix RT-PCR Master mix, 400 nM of each NLN primer, 1 μM NLN probe, 3.6 μL of DEPC H_2O and 4 μL of cDNA template. The RT-PCR program was performed under the following conditions: 95 °C for 3 min followed by 45 cycles of 95 °C for 3 s and 60 °C for 30 s.

2.3. hMPV detection using IFA

The specimens from clinical patients were washed three times with phosphate-buffered saline (PBS) solution. The respiratory epithelial cells were then centrifuged at 2000 rpm for 10 min, and the supernatant was discarded. An appropriate volume of PBS solution was added, and the sample solution was mixed. The epithelial cells were spotted onto slides, and the cell smears were air-dried and fixed in cold acetone for 10 min. The cell smears were incubated for 30 min at 37 °C with a FITC-labeled D^3 DFA Metapneumovirus Identification Kit (Diagnostic Hybrids, Athens, OH, USA). After incubation, the cells were washed three times in PBS solution for 10 min, air-dried and mounted with mounting media. The slides were viewed and evaluated using a fluorescence microscope (Olympus Optical, Hamburg, Germany), and the IFA data were used to assess the detection of hMPV-infected cells in the specimens.

2.4. Optical setup of HT-MEFB

In HT-MEFB, a He–Ne laser (17 mW, 632.8 nm, Newport) was used as the excitation light source. The intensity of the laser beam was modulated at a frequency of 1 kHz using a chopper. A beam splitter was applied to split the laser beam into a signal beam and a reference beam. The intensity-modulated signal beam was directed incident to each well of a 96-well immunoplate to measure the antigen–antibody interaction. The immunocomplexes were placed on the bottom of the immunoplate wells. Two identical long-pass filters (cutoff wavelength = 640 nm) were introduced into the instrument to detect the intensity-modulated fluorescence signal via a photomultiplier tube (PMT). Two lock-in amplifiers were used

to simultaneously measure the magnitude of the laser intensity from the reference channel and the fluorescence signal from the signal channel for hMPV detection.

2.5. hMPV detection using HT-MEFB

The polyclonal antibody (anti-hMPV) used as the capture and detection antibodies in this study was provided by Department of Laboratory Medicine, Linkou Chang Gung Memorial Hospital, Taoyuan, Taiwan. Bovine serum albumin (BSA) and PBS were purchased from Sigma (St. Louis, MO, USA). GNP-conjugated streptavidin (Au-SA, GNP diameter ~40 nm) was obtained from Innova Biosciences (Cambridge, UK), and Cy5-PEG-biotin (MW: 1000, length: ~7 nm) was purchased from Nanocs (New York, NY, USA). Lastly, the 96-well immunoplates were obtained from Corning Costar (Corning, NY, USA).

Briefly, 96-well immunoplates were first coated with 100 μL of 3 μg/mL (300 ng/well) capture antibody (anti-hMPV) at 37 °C for 2 h. The plates were then washed six times with PBS solution. After the immunoplates were blocked with 100 μL of 2% BSA in PBS solution (2% BSA–PBS) for 1 h at 37 °C, 25-fold dilutions of the UV-irradiated clinical samples in a total volume of 100 μL were individually added to the wells, and the plates were incubated at 37 °C for 2 h. The immunoplates were then washed six times with PBS solution. Subsequently, 100 μL of 2 μg/mL biotinylated detection antibody solution was added to each well, and the plates were then incubated for 1 h at 37 °C to form the capture antibody/target/biotinylated detection antibody immunocomplex. After immunocomplex formation, each well was washed six times with PBS solution. The immunoplates were then incubated with 100 μL of Au-SA in PBS solution (9×10^9 mL^{-1}) for 0.5 h at 37 °C, and 100 μL of 10 μM Cy5-PEG-biotin solution was added to each well. The plates were then incubated at 37 °C for 0.5 h. After washing six times with PBS solution, the fluorescence of each well of the immunoplate was measured by HT-MEFB. A schematic diagram of the experimental procedures is shown in Fig. 1. This assay was conducted in parallel using a conventional 96-well immunoplate, requiring a scanning time of 15 min for all 96 wells.

2.6. Statistical analysis

The statistical analyses were performed using Student's *t*-test to determine the *p* values and 95% confidence intervals (95% CIs). Following the criteria for optimal discrimination described previously, the receiver operating characteristics (ROC) curve was used to determine the correlation between the level of the measured fluorescence signal and the patient infection status. The area under the ROC curve (AUC) was calculated to determine whether the platform is suitable for detecting hMPV. Larger AUC values indicate better performance of the diagnostic platform in discriminating diseased and non-diseased subjects.

3. Results

3.1. hMPV detection using PCR-based assay

Currently, RT-PCR is the most sensitive, specific and frequently used diagnostic method for hMPV detection. In this study, 91 clinical samples from children of less than 3 years of age were tested for hMPV infection using the PCR-based assay. The results of this assay showed that 31 samples were positive and 60 samples were negative for hMPV. For the purposes of this study, the results from the PCR-based assay are used as the gold standard for comparison with other methods.

3.2. hMPV detection using IFA

The immunofluorescence staining of cells from nasopharyngeal secretions offers advantages in some laboratory settings and should produce more rapid results than PCR-based assays. IFA is therefore commonly used in clinical virology laboratories for the diagnosis of respiratory viruses. In this experiment, 91 clinical samples were tested using IFA. Of the 31 PCR-positive samples, 18 samples were found to be hMPV-positive and 13 samples were found to be hMPV-negative using IFA. All of the 60 samples that tested negative for hMPV by the PCR-based assay also tested negative using IFA. According to these results, the sensitivity (true positive) and specificity (true negative) of IFA were 58.1% and 100%, respectively. In addition, the accuracy and false-negative predictive value (one minus negative predictive value) of IFA were estimated to be 85.7% and 17.8%, respectively.

We then separately analyzed the experimental results of the 55 SP and 36 nasopharyngeal aspirate specimens. Using the 55 SP samples, a sensitivity of 56.3% and a specificity of 100% were reached with IFA for hMPV diagnosis. In addition, the accuracy and false-negative predictive value were estimated to be 87.3% and 15.2%, respectively. Moreover, using the 36 nasopharyngeal aspirate samples, the sensitivity and the specificity were 60.0% and 100%, respectively. The accuracy was 83.3%, and the false-negative predictive value was 22.2%. These analytical results are shown in Table 2.

3.3. Measurement of hMPV using HT-MEFB

To develop a highly sensitive assay for hMPV detection, we analyzed the HT-MEFB platform to determine its sensitivity and specificity using 91 clinical samples. Twenty-five-fold dilutions of the UV-irradiated samples were added to a 96-well immunoplate to form a <capture antibody/target/MEF probe> immunocomplex.

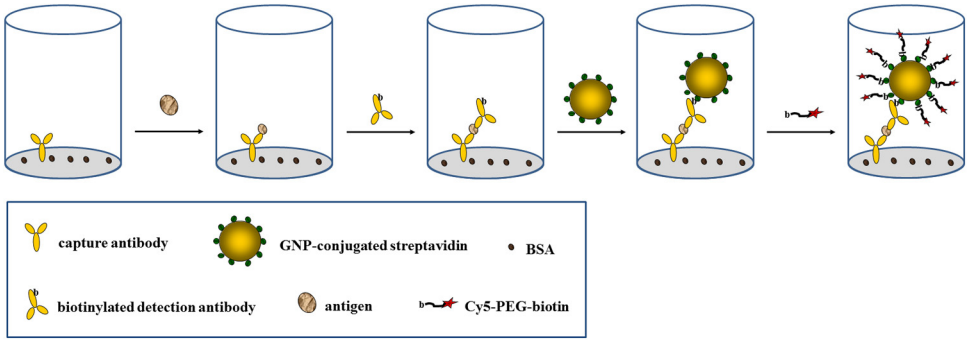

Fig. 1. Schematic diagram of the experimental procedures.

Table 2
Comparison of the performances of HT-MEFB and IFA with different types of samples.

		HT-MEFB	IFA
All samples (*including 55 SP and 36 nasopharyngeal aspirate samples*)	Sensitivity	77.4% (24/31)	58.1% (18/31)
	Specificity	91.7% (55/60)	100% (60/60)
	Accuracy	86.8% (79/91)	85.7% (78/91)
	False-negative predictive value	11.3% (7/62)	17.8% (13/73)
55 SP samples	Sensitivity	87.5% (14/16)	56.3% (9/16)
	Specificity	92.3% (36/39)	100% (39/39)
	Accuracy	90.9% (50/55)	87.3% (48/55)
	False-negative predictive value	5.3% (2/38)	15.2% (7/46)
36 nasopharyngeal aspirate samples	Sensitivity	73.3% (11/15)	60.0% (9/15)
	Specificity	85.7% (18/21)	100% (21/21)
	Accuracy	80.6% (29/36)	83.3% (30/36)
	False-negative predictive value	18.2% (4/22)	22.2% (6/27)

Table 3
Sensitivity and specificity obtained for different cutoff values of the normalized hMPV level.

Cutoff level (a.u.)	Sensitivity (%)	Specificity (%)
0.7736	83.87	80.00
0.9069	77.42	91.67
1.008	70.79	95.00

According to our previous study, HT-MEFB can use non-diluted or 10×-diluted clinical specimens, and the results show similar detection sensitivity and specificity compared with the analyte in PBS buffer. This finding implies that the uncertainties and accuracy are consistent to each other and that no significant differences are obtained between diluted and non-diluted clinical specimens (Chang et al., 2009; Huang et al., 2009). The intensity-modulated fluorescence signal from the bound MEF probe in each well was measured. The normalized hMPV levels in the control group ($n = 60$) were compared to those found for the hMPV-positive patients ($n = 31$), as shown in Fig. 2(a). Each sample represents the mean of five measurements. The results are presented using the normalized hMPV level, which was defined as the measured fluorescence intensity from each well normalized to the fluorescence intensity of the positive controls in the same plate. Thus, the normalized hMPV level is presented in arbitrary units (a.u.). The results showed that the normalized hMPV level found for the hMPV-positive group was significantly higher than that found for the control group. Additionally, both the mean and median values of the normalized hMPV levels found for hMPV-positive patients (2.6 and 1.2, respectively) were markedly higher than those found for the control group (0.6 and 0.6, respectively).

To identify the criteria that would enable optimal discrimination, we used a fitting program (kindly provided by John Eng ROC analysis, web-based calculator for ROC curve, Johns Hopkins University, Baltimore, MD, USA; http://www.jrocfit.org.) to calculate the ROC curve based on the maximum fit of a binomial model. Fig. 2(b) shows the empirical and fitted ROC curves of the 91 samples, and the AUC values were 0.866 (95% confidence interval: 0.772–0.961) and 0.861, respectively. The ROC curve is a graphical plot of the sensitivity as a function of the false positive rate (one minus specificity) for a binary classification system as the discrimination threshold is varied. Furthermore, each point on the ROC curve corresponds to a unique pair of sensitivity and specificity values. In this study, based on the empirical ROC curve, we calculated the sensitivity and specificity for different cutoff values of the normalized hMPV level, as shown in Table 3. The selection of 0.9069 as the cutoff level resulted in an accuracy and false-negative predictive value of HT-MEFB for hMPV detection greater than 86.8% and less than 11.3%, respectively.

Furthermore, we individually analyzed the 55 SP and 36 nasopharyngeal aspirate samples utilizing the ROC curve. First, we only selected the 55 SP samples as the analyzed specimen. The normalized hMPV levels obtained for the control group ($n = 39$) were compared to those obtained for the hMPV-positive patients ($n = 16$), as shown in Fig. 3(a), and the AUCs of the empirical and fitted ROC curves were 0.950 (95% confidence interval: 0.897–1.000) and 0.951, respectively, as shown in Fig. 3(b). The selection of a normalized hMPV level of 0.9203 as the cutoff value resulted in a sensitivity of 87.5% and a specificity of 92.3% for hMPV diagnosis

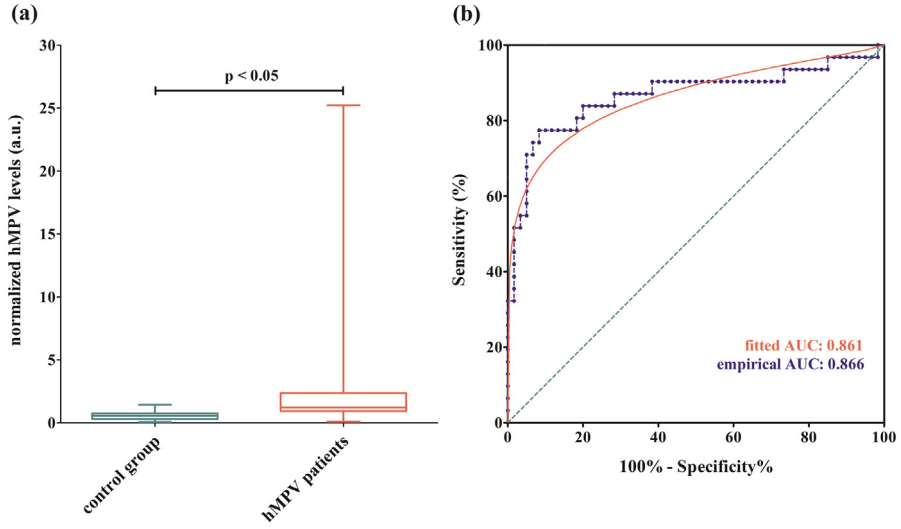

Fig. 2. (a) The normalized hMPV levels in the control group ($n = 60$) were compared to those in the hMPV-positive patients ($n = 31$). The middle line in the rectangle represents the median. The lower and upper boundaries of the rectangle are the 25th and 75th percentiles, respectively. The ends of the whiskers are the minimum and maximum values of the data. (b) ROC curve analysis of HT-MEFB for the discrimination of hMPV-positive patients from the 91 clinical samples. The empirical ROC curve (blue) and fitted ROC curve (red) and their AUC values of 0.866 (95% confidence interval: 0.772–0.961) and 0.861, respectively, are shown. (For interpretation of reference to color in this figure legend, the reader is referred to the web version of this article.)

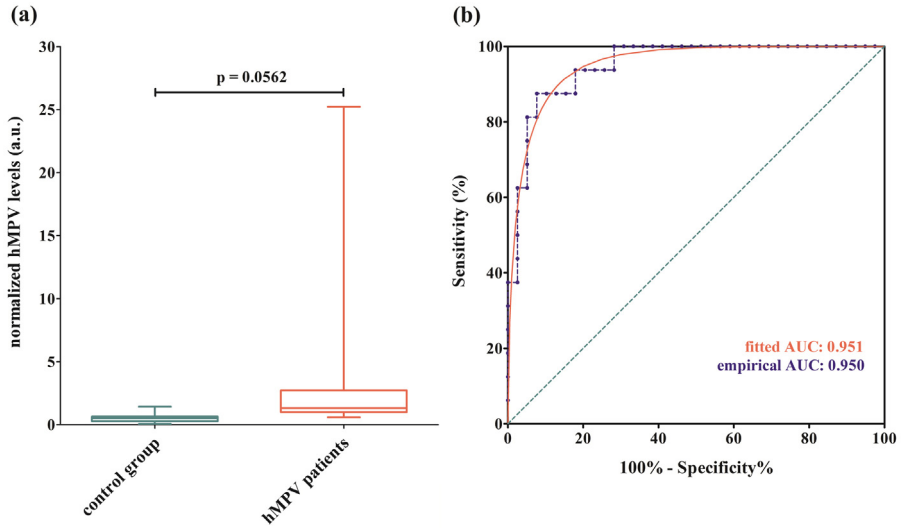

Fig. 3. Results obtained using the 55 SP samples as the analyzed specimen. (a) The normalized hMPV levels in the control group ($n = 39$) were compared to those in the hMPV-positive patients ($n = 16$). The middle line in the rectangle shows the median. The lower and upper boundaries of the rectangle are the 25th and 75th percentiles, respectively. The ends of the whiskers are the minimum and maximum values of the data. (b) ROC curve analysis of HT-MEFB for the discrimination of hMPV-positive patients from the 55 SP samples. The empirical ROC curve (blue) and fitted ROC curve (red) and their AUC values of 0.950 (95% confidence interval: 0.897–1.000) and 0.951, respectively, are shown. (For interpretation of reference to color in this figure legend, the reader is referred to the web version of this article.)

using HT-MEFB. The accuracy and false-negative predictive value were estimated to be 90.9% and 5.3%, respectively.

In contrast, the selection of only 36 nasopharyngeal aspirate samples as the analyzed specimen resulted in the distributions of the normalized hMPV levels of hMPV-positive group ($n = 15$) and control group ($n = 21$) shown in Fig. 4(a) and (b), respectively, with AUCs of the empirical and fitted ROC curves of 0.771 (95% confidence interval: 0.584–0.959) and 0.766, respectively. The sensitivity and specificity were 73.3% and 85.7%, respectively. The accuracy was estimated to be 80.6%, and the false-negative predictive value was 18.2%. These results are shown in Table 2 and indicate that SP samples may be more suitable for use with this proposed platform compared with nasopharyngeal aspirate samples. This difference may be observed because the collection and manipulation of specimens will influence the matrix effects to result in different accuracies.

4. Discussion

The relatively high incidence of hMPV leads to the need for a reliable and easy-to-use diagnostic tool (Huang et al., 2014). RT-PCR is normally the most effective and frequently used method for hMPV diagnosis. However, a PCR-based assay requires a well-trained technician several hours to acquire results and uses more expensive instruments (Kikuta et al., 2008; Wang et al., 2012). In contrast, IFA is another hMPV diagnostic method that is commonly used in clinical virology laboratories but requires a well-trained technician to analyze the staining results (Kikuta et al., 2008). In addition, according to the analysis performed in this study, the sensitivity and false-negative predictive value of IFA are 58.06% and 17.81%, respectively. Thus, the development of a novel platform for hMPV diagnosis is encouraged. In this study, HT-MEFB shows a 20% increase in detection sensitivity compared with IFA, although

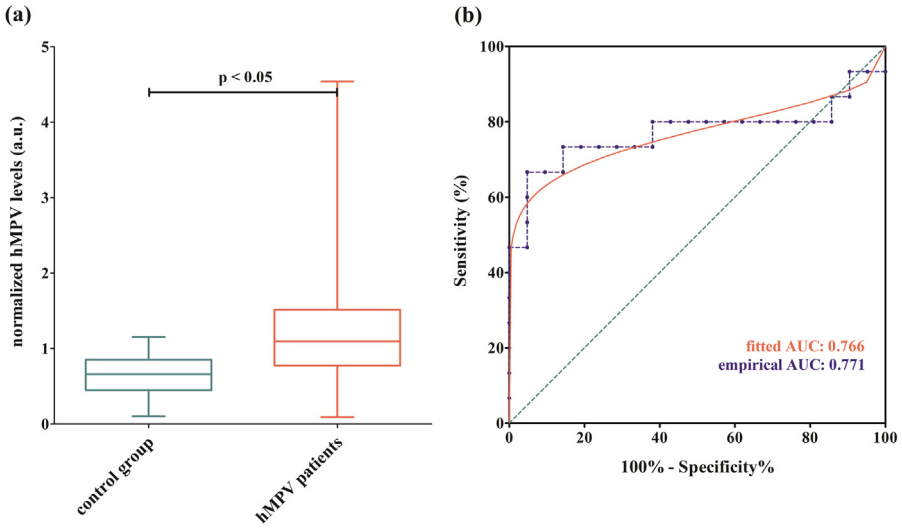

Fig. 4. Results obtained using the 36 nasopharyngeal aspirate samples as the analyzed specimen. (a) The normalized hMPV levels in the control group ($n = 21$) were compared to those in the hMPV-positive patients ($n = 15$). The middle line in the rectangle is the median. The lower and upper boundaries of the rectangle are the 25th and 75th percentiles, respectively. The ends of the whiskers are the minimum and maximum values of the data. (b) ROC curve analysis of HT-MEFB for the discrimination of hMPV-positive patients from the 36 nasopharyngeal aspirate samples. The empirical ROC curve (blue) and fitted ROC curve (red) and their AUC values of 0.771 (95% confidence interval: 0.584–0.959) and 0.766, respectively, are shown. (For interpretation of reference to color in this figure legend, the reader is referred to the web version of this article.)

the measured specificities of IFA and HT-MEFB are 100% and 91.7%, respectively. However, the false-negative predictive value of HT-MEFB (11.3%) is markedly lower than that obtained for IFA (17.8%). Moreover, if we focus on the 55 SP samples, the accuracy of HT-MEFB reached 90.9%, and the detection sensitivity reached 87.5%. These performances are very close to those obtained with different detection platforms, such as enzyme-based immunoassay and ICA for different purposes (Kikuta et al., 2008; Kukavica-Ibrulj and Boivin, 2009).

In this study, HT-MEFB was developed as a cost-effective method with high-throughput capability and adequate sensitivity for clinical hMPV diagnosis. Two identical polyclonal antibodies in the sandwich immunoassay were used in the system, which not only increases the availability of the antibody but also makes the method cost-effective for clinical diagnosis. Because of the need for high-throughput scanning, HT-MEFB integrates a conventional 96-well immunoplate into the platform, which exhibits a significant advantage in comparison with other GNP-based detection systems, such as GNP scattering. Because the HT-MEFB is based on 96-well immunoplates, it can be used for parallel assays and is thus able to significantly improve the measurement efficiency. In this study, a scanning rate of <15 min for 96 samples was properly conducted. Moreover, HT-MEFB shows high detection sensitivity because a 96-well-designed MEF probe is used in the sandwich immunoassay. Based on the MEF effect and the optimized number of fluorophores attached to a single MEF probe, the fluorescence signal can be significant enhanced experimentally, and the sandwich immunoassay with HT-MEFB may provide a method with high bio-specificity and sensitivity for clinical hMPV diagnosis.

Acknowledgments

This research was supported by the Linkou Chang Gung Memorial Hospital through the research grants CMRPD290091 and CMRPD290092 and by the National Science Council, Taiwan (NMRPG376301). Support from The Ministry of Education, Taiwan through the Aiming for the Top University Plan (EMRPD1B0251 and EMRPD1B0301) is also appreciated.

References

Baptista, P., Pereira, E., Eaton, P., Doria, G., Miranda, A., Gomes, I., Quaresma, P., Franco, R., 2008. Gold nanoparticles for the development of clinical diagnosis methods. Anal. Bioanal. Chem. 391, 943–950.

Chang, Y.F., Chen, R.C., Lee, Y.J., Chao, S.C., Su, L.C., Li, Y.C., Chou, C., 2009. Localized surface plasmon coupled fluorescence fiber-optic biosensor for alpha-fetoprotein detection in human serum. Biosens. Bioelectron. 24, 1610–1614.

Chang, Y.F., Hung, S.H., Lee, Y.J., Chen, R.C., Su, L.C., Lai, C.S., Chou, C., 2011. Discrimination of breast cancer by measuring prostate-specific antigen levels in women's serum. Anal. Chem. 83, 5324–5328.

Chang, Y.F., Wang, S.F., Huang, J.C., Su, L.C., Yao, L., Li, Y.C., Wu, S.C., Chen, Y.M., Hsieh, J.P., Chou, C., 2010. Detection of swine-origin influenza A (H1N1) viruses using a localized surface plasmon coupled fluorescence fiber-optic biosensor. Biosens. Bioelectron. 26, 1068–1073.

Chang, Y.F., Yu, J.S., Chang, Y.T., Su, L.C., Wu, C.C., Chang, Y.S., Lai, C.S., Chou, C., 2013. The utility of a high-throughput scanning biosensor in the detection of the pancreatic cancer marker ULBP2. Biosens. Bioelectron. 41, 232–237.

Chao, C.-H., Chang, Y.-F., Chen, H.-C., Lin, L.-Y., Yu, P.-C., Chang, Y.-S., Lee, Y.-J., Chou, C., 2012. Detection of urine cofilin-1 from patients hospitalized in the intensive care unit using the metal-enhanced fluorescence technique. Sens. Actuator B: Chem. 173, 184–190.

Chen, S.H., Hsu, Y.P., Lu, H.Y., Ho, J.A., 2014. Gold/phospholipid nanoconstructs as label-free optical probes for evaluating phospholipase A2 activity. Biosens. Bioelectron. 52, 202–208.

Ebihara, T., Endo, R., Kikuta, H., Ishiguro, N., Ishiko, H., Hara, M., Takahashi, Y., Kobayashi, K., 2004. Human metapneumovirus infection in Japanese children. J. Clin. Microbiol. 42, 126–132.

Ebihara, T., Endo, R., Ma, X.M., Ishiguro, N., Kikuta, H., 2005. Detection of human metapneumovirus antigens in nasopharyngeal secretions by an immunofluorescent-antibody test. J. Clin. Microbiol. 43, 1138–1141.

Fenwick, F., Young, B., McGuckin, R., Robinson, M.J., Taha, Y., Taylor, C.E., Toms, G.L., 2007. Diagnosis of human metapneumovirus by immunofluorescence staining with monoclonal antibodies in the North-East of England. J. Clin. Virol. 40, 193–196.

Geddes, C.D., Gryczynski, I., Malicka, J., Gryczynski, Z., Lakowicz, J.R., 2003. Metal-enhanced fluorescence: potential applications in HTS. Comb. Chem. High Throughput Screen 6, 109–117.

Hsieh, B.Y., Chang, Y.F., Ng, M.Y., Liu, W.C., Lin, C.H., Wu, H.T., Chou, C., 2007. Localized surface plasmon coupled fluorescence fiber-optic biosensor with gold nanoparticles. Anal. Chem. 79, 3487–3493.

Huang, C.G., Tsao, K.C., Lin, T.Y., Huang, Y.C., Lee, L.A., Chen, T.H., Huang, Y.L., Shih, S.R., 2010. Estimates of individuals exposed to human metapneumovirus in a community-based Taiwanese population in 1999. Arch. Virol. 155, 343–350.

Huang, J.C., Chang, Y.F., Chen, K.H., Su, L.C., Lee, C.W., Chen, C.C., Chen, Y.M., Chou, C., 2009. Detection of severe acute respiratory syndrome (SARS) coronavirus nucleocapsid protein in human serum using a localized surface plasmon coupled fluorescence fiber-optic biosensor. Biosens. Bioelectron. 25, 320–325.

Huang, Y., Shi, M., Zhao, L.M., Zhao, S.L., Hu, K., Chen, Z.F., Chen, J., Liang, H., 2014. Carbon nanotube signal amplification for ultrasensitive fluorescence polarization detection of DNA methyltransferase activity and inhibition. Biosens. Bioelectron. 54, 285–291.

Ingram, R.E., Fenwick, F., McGuckin, R., Tefari, A., Taylor, C., Toms, G.L., 2006. Detection of human metapneumovirus in respiratory secretions by reverse-transcriptase polymerase chain reaction, indirect immunofluorescence, and virus isolation in human bronchial epithelial cells. J. Med. Virol. 78, 1223–1231.

Ishiguro, N., Ebihara, T., Endo, R., Ma, X., Shirotsuki, R., Ochiai, S., Ishiko, H., Kikuta, H., 2005. Immunofluorescence assay for detection of human metapneumovirus-specific antibodies by use of baculovirus-expressed fusion protein. Clin. Diagn. Lab. Immunol. 12, 202–205.

Janssen, K., Flore, K., Piette, A., Vankeerberghen, A., Padalko, E., 2010. Implementation of real-time RT-PCR for detection of human metapneumovirus and its comparison with enzyme immunoassay. Arch. Virol. 155, 207–215.

Kikuta, H., Sakata, C., Gamo, R., Ishizaka, A., Koga, Y., Konno, M., Ogasawara, Y., Sawada, H., Taguchi, Y., Takahashi, Y., Yasuda, K., Ishiguro, N., Hayashi, A., Ishiko, H., Kobayashi, K., 2008. Comparison of a lateral-flow immunochromatography assay with real-time reverse transcription-PCR for detection of human metapneumovirus. J. Clin. Microbiol. 46, 928–932.

Klemenc, J., Asad Ali, S., Johnson, M., Tollefson, S.J., Talbot, H.K., Hartert, T.V., Edwards, K.M., Williams, J.V., 2012. Real-time reverse transcriptase PCR assay for improved detection of human metapneumovirus. J. Clin. Virol.: Off. Publ. Pan American Soc. Clin. Virol. 54, 371–375.

Kukavica-Ibrulj, I., Boivin, G., 2009. Detection of human metapneumovirus antigens in nasopharyngeal aspirates using an enzyme immunoassay. J. Clin. Virol. 44, 88–90.

Landry, M.L., Cohen, S., Ferguson, D., 2008. Prospective study of human metapneumovirus detection in clinical samples by use of light diagnostics direct immunofluorescence reagent and real-time PCR. J. Clin. Microbiol. 46, 1098–1100.

Landry, M.L., Ferguson, D., Cohen, S., Peret, T.C., Erdman, D.D., 2005. Detection of human metapneumovirus in clinical samples by immunofluorescence staining of shell vial centrifugation cultures prepared from three different cell lines. J. Clin. Microbiol. 43, 1950–1952.

Lin, P.-Y., Lin, T.-Y., Huang, Y.-C., Taso, K.-C., Huang, Y.-L., 2005. Human metapneumovirus and community-acquired pneumonia in children. Chang Gung Med. J. 28, 683–688.

Matsuzaki, Y., Takashita, E., Okamoto, M., Mizuta, K., Itagaki, T., Katsushima, F., Katsushima, Y., Nagai, Y., Nishimura, H., 2009. Evaluation of a new rapid antigen test using immunochromatography for detection of human metapneumovirus in comparison with real-time PCR assay. J. Clin. Microbiol. 47, 2981–2984.

Morton, S.M., Silverstein, D.W., Jensen, L., 2011. Theoretical studies of plasmonics using electronic structure methods. Chem. Rev. 111, 3962–3994.

Okamoto, M., Sugawara, K., Takashita, E., Muraki, Y., Hongo, S., Mizuta, K., Itagaki, T., Nishimura, H., Matsuzaki, Y., 2010. Development and evaluation of a whole virus-based enzyme-linked immunosorbent assay for the detection of human metapneumovirus antibodies in human sera. J. Virol. Methods 164, 24–29.

van den Hoogen, B.G., de Jong, J., Groen, J., Kuiken, T., de Groot, R., Fouchier, R.A.M., Osterhaus, A., 2001. A newly discovered human pneumovirus isolated from young children with respiratory tract disease. Nat. Med. 7, 719–724.

Wang, X., Zhang, Q., Zhang, F., Ma, F.L., Zheng, W.Z., Zhao, Z.H., Bai, Y.L., Zheng, L.S., 2012. Visual detection of the human metapneumovirus using reverse transcription loop-mediated isothermal amplification with hydroxynaphthol blue dye. Virol. J. 9, 6.

Wei, H.Y., Tsao, K.C., Huang, C.G., Huang, Y.C., Lin, T.Y., 2013. Clinical features of different genotypes/genogroups of human metapneumovirus in hospitalized children. J. Microbiol. Immunol. Infect. 46, 352–357.

Williams, J.V., Harris, P.A., Tollefson, S.J., Halburnt-Rush, L.L., Pingsterhaus, J.M., Edwards, K.M., Wright, P.F., Crowe, J.E., 2004. Human metapneumovirus and lower respiratory tract disease in otherwise healthy infants and children. N. Engl. J. Med. 350, 443–450.